DALTON

A route to the dispersion of ultrafine cobalt particles on zeolite Na–X through salt occlusion and reduction†

Itasham Hussain,[a] Ian Gameson,[a] Paul A. Anderson,[a] Marcin Slaski,[b] Peter P. Edwards *,[a] and Alan Dyer[c]

[a] *School of Chemistry, University of Birmingham, Edgbaston, Birmingham B15 2TT, UK*
[b] *School of Physics and Space Research, University of Birmingham, Edgbaston, Birmingham B15 2TT UK*
[c] *Department of Pure and Applied Chemistry, University of Salford, Salford M15 4WT, UK*

Ultrafine magnetic cobalt particles, encapsulated within a zeolitic host, have been prepared *via* the seldom-used method of salt occlusion followed by reduction to the metallic state. Powder X-ray diffraction and electron microscopy clearly showed the formation of 150–250 Å cobalt particles which were too large to be contained in the supercage of the zeolite. An increase in cobalt content increases the number of these cobalt particles, but not their size. We thus propose that these particles are encapsulated within locally distorted areas of the zeolite structure. This work demonstrates the clear potential of zeolites as templates or host matrices for the synthesis of ultrafine metal particles.

At the present time there is considerable interest in the study of ultrafine magnetic particles.[1–10] The many potential applications, especially in the area of high-density recording media, guarantee an increasing technological interest,[5–10] while forefront scientific issues relating to size effects in the electronic properties of small particles continue to underpin all investigations.[11] We are currently exploring a range of synthetic options aimed at the controlled fabrication of composite materials[9,12] containing ultrafine magnetic and non-magnetic constituents. Our ultimate goal is to 'engineer' composite materials with specific properties ranging from those of the bulk magnetic constituent to those which can be identified with the finite size of the incorporated magnetic structure.

Here we hope to illustrate the great potential of zeolites[13,14] as templates and hosts for the preparation of ultrafine magnetic particles, in this instance of cobalt metal. In particular, the little known process of 'salt occlusion' with subsequent reduction offers great scope for a high degree of control of both the dimensions and concentration of ultrafine cobalt particles.

Over the past couple of decades, much effort has been directed toward the use of zeolites as host and support materials for the preparation of small metallic clusters and particles.[14–16] Much of this interest has arisen from the important requirement to produce highly dispersed, efficient and selective catalysts for a wide range of chemical processes.[15] In contrast, the study of the electronic properties of such materials is still in its infancy.[14]

Metal atoms (acknowledged[14] to be initiators of cluster and particle formation) may be introduced in the form of vapours (in the case of the low boiling point elements) or as volatile compounds.[13–16] The latter, after sorption, are subsequently decomposed by heat treatments (*e.g.* metal carbonyls). Perhaps the most widely used route for metal particle formation involves ion exchange (which almost exclusively takes place in aqueous solution) followed by reduction, leading to the formation of small metal clusters[14] (in the present case, for cobalt metal) *via* reaction (1).[17] Heating to high temperatures then produces

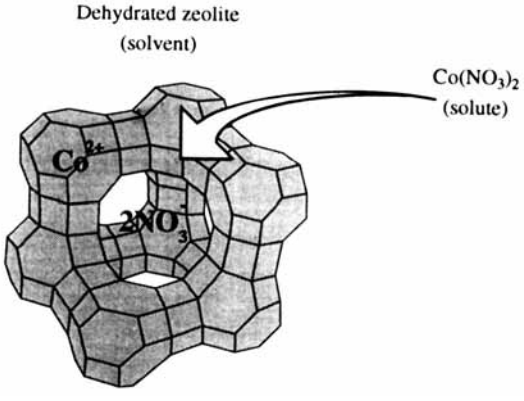

Fig. 1 Schematic representation of the occlusion of cobalt nitrate into zeolite Na–X

$$Co^{II}\ \text{zeolite} + H_2 \xrightarrow{\text{Heat}} H\ \text{zeolite} + Co^0 \qquad (1)$$

clustering to form small metal particles. There are, however, major limitations in this approach if one is seeking to form a high concentration of spatially dispersed clusters and uniform ultrafine particles. For example, strictly controlled conditions (*e.g.* pH control) have to be rigorously enforced during ion exchange in aqueous solutions in order to avoid hydrolysis and crystal damage.[18]

Here we draw attention to, and utilise, the method of 'occlusion' of metal salts in zeolites as a starting point for our synthesis of ultrafine cobalt particles. This process, pioneered by Barrer and Meier,[19,20] involves the occlusion (or incorporation) of salt molecules and aggregates of such molecules within the intracrystalline cavities and voids in zeolites. To effect occlusion, dehydrated zeolites are heated with metal salts (or their vapours). The sorbed salt molecules (the solute) are effectively dispersed or 'dissolved' by the zeolite (the solvent), with both occluded cations and anions finding specific binding sites within the interior cavities and voids of the host matrix. A schematic representation of the occlusion process is shown in Fig. 1; here the dehydrated zeolite takes the role of a solid polar solvent and the occluded metal salt (in this case cobalt nitrate) the incoming solute.

† Basis of the presentation given at Dalton Discussion No. 1, 3rd–5th January 1996, University of Southampton, UK.

Non-SI unit employed: emu = SI × $10^6/4\pi$.

The break-up (or dissolution) of the occluded salt arises because of the very large electrostatic fields existing within the zeolite host structure.[21] In the present instance, we find that careful decomposition of occluded cobalt nitrate samples, followed by reduction with a hydrogen–argon mixture, produces high concentrations of dispersed, ultrafine cobalt particles on (and within) the zeolite crystallite. It appears that the characteristic zeolite host structure plays an important role not only in the initial cluster formation but also in the resultant dispersion of ultrafine particles. We present here our results on the synthesis, structural characterisation and magnetic properties of these composite materials.

Experimental

Synthesis

To effect the occlusion of cobalt in the form of a salt, cobalt nitrate was chosen because of its relatively low melting point (57 °C) and the ease with which it can be purified. Furthermore, the low decomposition temperature (72 °C) for conversion to the oxide (Co_3O_4), and ultimately to the metal, means that the formation of occluded oxide can be carried out at a relatively low temperature to minimise any possible decomposition of the host zeolite framework. Stoichiometric amounts of analytical grade $Co(NO_3)_2{\cdot}6H_2O$ (pink powder), supplied by Aldrich Chemicals and zeolite Na–X, $Na_{86}(AlO_2)_{86}(SiO_2)_{106}{\cdot}264H_2O$ (white powder), supplied by Laporte Inorganics, were intimately ground together using a mortar and pestle. This mixture was then transferred to a controlled atmosphere furnace system for subsequent synthesis. The occluded sample was prepared by slowly heating the mixture (under a dynamic of vacuum 10^{-3} Pa) to a temperature of 60 °C. The occluded cobalt nitrate sample was turquoise blue, while the subsequent occluded oxide material exhibits a grey colour. The infrared spectrum of the occluded nitrate phase shows a characteristic vibrational mode from the individual nitrate ion at *ca.* 1385 cm^{-1}. This fingerprint spectrum is absent from the spectrum of the material heated above 200 °C, indicating the decomposition of the occluded nitrate species. X-Ray diffraction (XRD) analysis of the occluded nitrate sample showed the pattern to be identical to pure Na–X; no cobalt nitrate peaks were visible. The mixture was then heated to a temperature of 550 °C for 12 h to ensure complete occlusion and then allowed to cool under vacuum. The sample was again heated to 550 °C, this time in a continuous flow of 35% H_2–Ar gas for 4 h, to produce a grey material. The resulting (reduced) product was then allowed to cool naturally in the furnace under a flowing nitrogen atmosphere. Samples containing a cobalt loading of 1, 5, 10, 15 and 20 atoms per unit cell of Na–X were prepared in this fashion. With regard to the composition of these materials, the following nomenclature will be adopted. A loading of one cobalt atom per unit cell of zeolite Na–X will be designated 1Co/Na–X. A similar notation will be applied to the successively loaded samples; the synthetic conditions for each sample will also be indicated, *i.e.* occluded/reduced.

Characterisation

The materials were examined by powder X-ray diffraction using a Siemens D5000 diffractometer fitted with a primary beam Ge monochromator (Cu-Kα1) and operating in transmission mode. The materials were also characterised by scanning transmission electron microscopy (STEM) using a JEOL-4000FX microscope in the standard side-entry configuration, equipped with a scanning pole piece and operated at 400 keV ($\approx 6.4 \times 10^{-14}$ J). The characteristic emission spectrum of each element was detected using EDAX (energy dispersive analysis by X-rays). Magnetic measurements were recorded from 4 to 300 K using a Cryogenics S100 (SQUID) susceptometer. ESR spectra were recorded on a Bruker ESP 300 spectrometer operating at X-band frequencies (*ca.* 9 GHz) with 100 kHz field modulation.

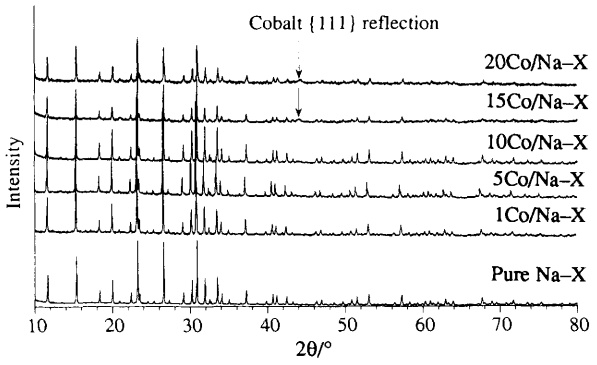

Fig. 2 X-Ray diffraction pattern of a sample of pure Na–X with successively loaded samples from 1Co/Na–X through to 20Co/Na–X-(occluded and reduced)

Results and Discussion

Powder X-ray diffraction

In Fig. 2 we show the XRD patterns of samples of zeolite Na–X loaded with one to twenty cobalt atoms per unit cell and reduced in the manner noted earlier. The lattice constant of Na–X is relatively unaffected by both the occlusion and subsequent reduction process, showing at most an expansion of some 0.5% [a = 25.05(1)–25.16(1) Å]. A similar lattice-constant expansion of 0.9% in zeolite Na–A has been reported by Barrer and Meier[20] upon occlusion with $AgNO_3$. This expansion in the latter system was accompanied by the formation of a superlattice arising from the ordering of the occluded species. We see no evidence from the XRD data in Fig. 2 for the formation of any such superlattice in this case of occluded $Co(NO_3)_2$.

It is apparent from these XRD patterns of the occluded and reduced samples that the overall integrity of the framework of the host zeolite has remained intact during the process of occlusion and subsequent reduction. There was no evidence from these patterns of either CoO or Co_3O_4. However, the increased cobalt loading of the sample is reflected in an increase in the fluorescence background observed in the X-ray pattern. At levels of loading beyond 5Co/Na–X, a broad reflection is observed at 2θ = 44.14°, which gradually increases in intensity with increasing cobalt loading (Fig. 2). The presence of this new reflection can be more clearly seen in Fig. 3, which is an expanded plot of the XRD data. This reflection corresponds to the most intense peak for the face-centred-cubic (fcc) form of cobalt.[22] Cobalt exists in two forms, at room temperature it has a hexagonal-close-packed (hcp) structure but this undergoes a phase change to fcc at about 450 °C. There is no evidence from our data for the presence of hcp cobalt. This is consistent with earlier work[23] which showed that fcc, unlike hcp as in the bulk metal, was the stable structure for cobalt particles.

Using the Scherrer equation,[24] it is possible to determine the mean diameter, L_{hkl}, of the cobalt particles from the observed XRD peak width at half-height, β_{hkl} (in radians), *via* equation (2), where λ is the X-ray wavelength, K is a constant (normally

$$L_{hkl} = \frac{K\lambda}{\beta_{hkl}\cos\theta} \qquad (2)$$

1) and 2θ is the position of the {hkl} reflection (in degrees).

The {111} cobalt reflections for 15Co/Na–X and 20Co/Na–X (Fig. 3) were fitted by a Gaussian profile to determine their peak widths at half-height. The Scherrer equation was then used to provide an estimate of particle size. For these samples, we determine average particle diameters of 150–250 Å. Such particle

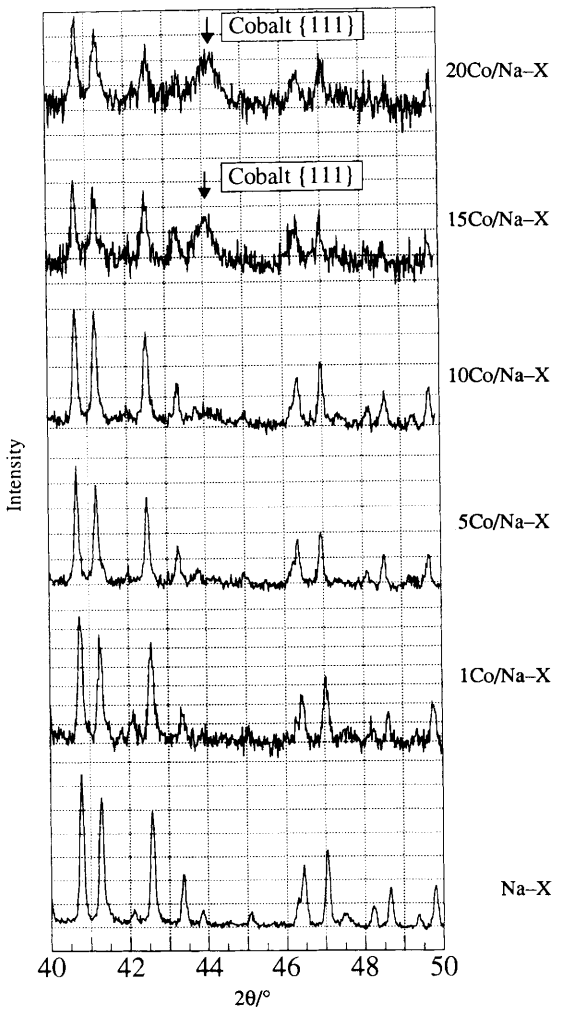

Fig. 3 Expanded X-ray diffraction patterns of each sample (2θ = 40–50°) showing the emergence of the cobalt {111} reflection

sizes are consistent with values observed in our STEM measurements, to which we now turn.

Scanning transmission electron microscopy

The occluded and reduced samples have been examined by STEM in order to establish the morphology, state of dispersion and particle size of the occluded and reduced component. The scanning electron image is particularly useful for observing the morphology of the zeolite crystals. In the transmission mode this technique enables a contrast to be highlighted between any metal particles which may be present and the host zeolite. EDAX was used to confirm the Si:Al ratio (1.3 ± 0.1:1) of the host Na–X both before and after occlusion. In addition, EDAX also confirmed the presence of cobalt both within the occluded and reduced samples of Na–X. As anticipated (see below) the spatial dispersion of elemental cobalt in the form of ultrafine particles is heterogeneous from grain to grain. This must be the case when occluded samples are reduced to form (local) high concentrations of atoms and clusters and then eventually ultrafine cobalt particles. Further, we will illustrate that, within a single grain, the growth process leading to the formation of a metal particle involves the diffusion of cobalt atomic and cluster species through the zeolite. This necessarily leaves certain regions of the zeolite depleted in metal content, while other regions will be cobalt-rich. For example, in the specific case of the sample 5Co/Na–X(occluded/reduced), cobalt EDAX over a number of particles (typically 10) gives an average cobalt content (per formula unit) of 8.2 ± 1.3. Mapping by the electron beam (typical beam size 10–50 nm)

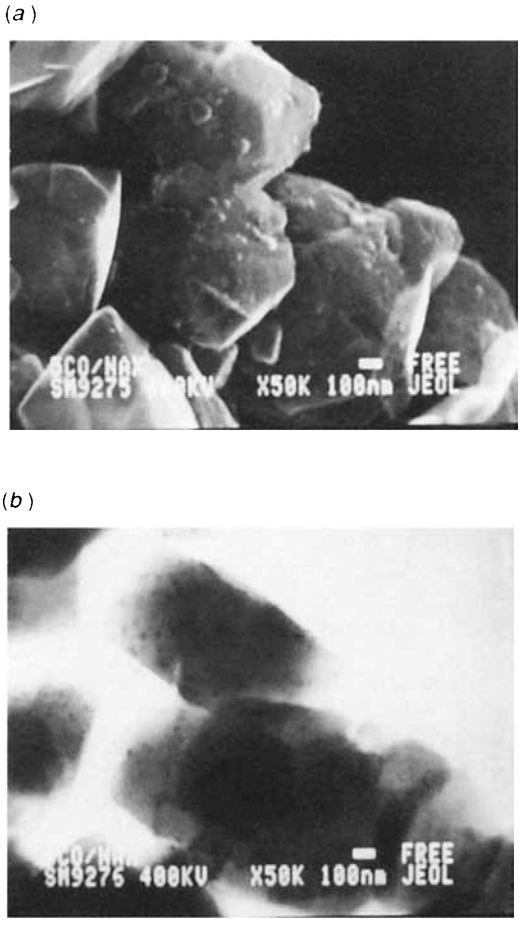

Fig. 4 (*a*) Scanning and (*b*) transmission electron micrograph of 5Co/Na–X(occluded/reduced)

reflects the heterogeneous concentration. Thus the value of 8.2 cobalt per unit cell implies that our analysis has perhaps concentrated too much on the particles (and regions of those particles) with locally high concentrations of cobalt at the expense of those grains (and regions) with fewer metal particles. With such a heterogeneous elemental distribution of cobalt, from cobalt-deficient regions to the cobalt particles themselves, such variations will be inevitable. However, this slightly higher than expected average cobalt content does lead us to conclude that no substantial loss of metal has occurred during the reduction process. We note also that the Si:Al content (*via* EDAX) is unchanged (within the experimental error of the technique) upon occlusion and reduction. These findings are representative of similar experiments on higher levels of cobalt loading.

STEM images of pure Na–X show that the material consists of irregular 1–2 μm cubic-type particles. Similar images are observed for the 1Co/Na–X(occluded/reduced) sample. However the presence of cobalt in the zeolite crystals of this low cobalt-loaded sample has been confirmed by EDAX. We thus conclude that for a loading of one cobalt per unit of Na–X only very small cobalt particles are formed within the zeolite host. This sample exhibits very weak ferromagnetism, as gauged by its response to an external magnet.

In Fig. 4(*a*) and 4(*b*) we show scanning and transmission electron micrographs, respectively, of a sample of 5Co/Na–X(occluded/reduced). One notes the emergence of the ultrafine cobalt metal particles of average diameter 150–200 Å which are easily observed as dark spots in the transmission image [Fig. 4(*b*)]. These are clearly too big to be accommodated within the supercage of the zeolite, some 13 Å in diameter. The presence of high concentrations of such particles on the external surfaces of the zeolite, some of which would inevitably lie approximately

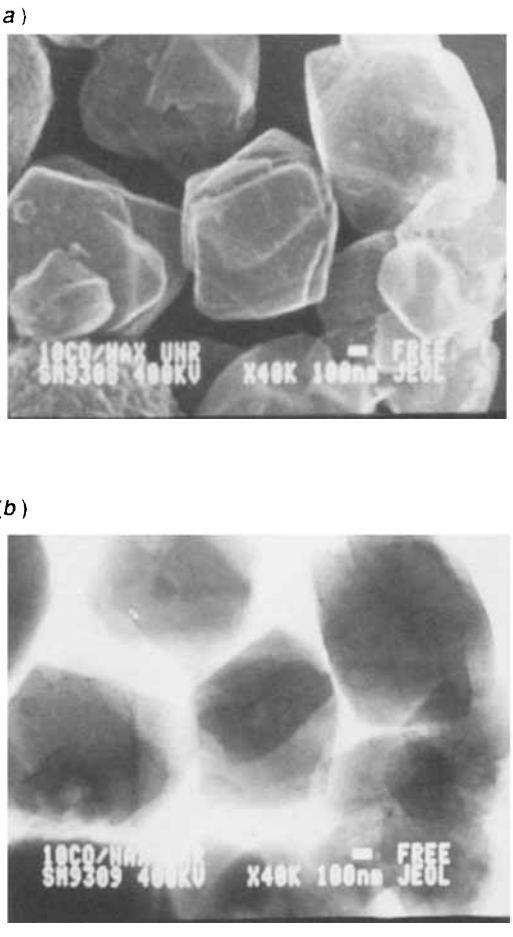

Fig. 5 (*a*) Scanning and (*b*) transmission electron micrograph of 10Co/Na–X(occluded)

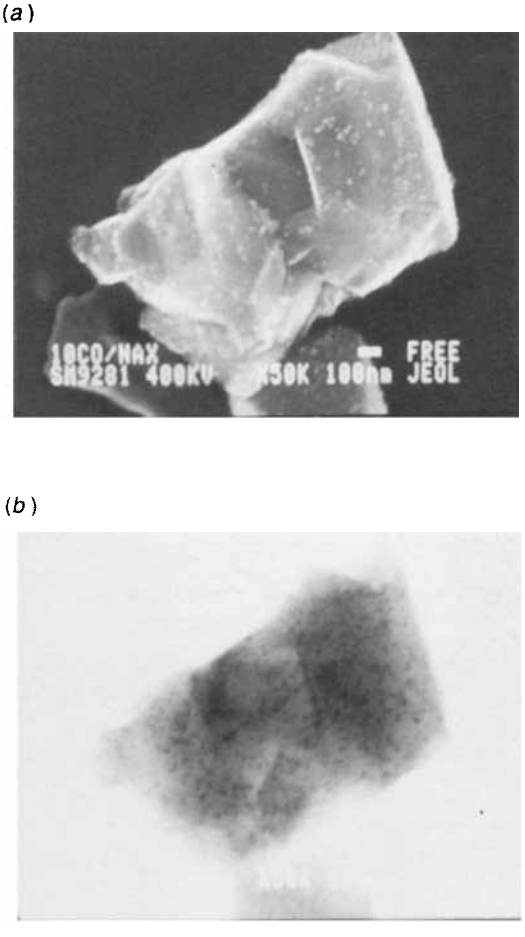

Fig. 6 (*a*) Scanning and (*b*) transmission electron micrograph of 10Co/Na–X(occluded/reduced)

parallel to the incoming electron beam, would give rise to a dark 'halo' around the transmission image of the zeolite grain. The noticeable absence of such an important feature in the TEM images of this sample (and indeed of higher cobalt-loaded samples) leads us to conclude that the majority of these particles are not present on the external surface of the zeolite, but appear to be located within the aluminosilicate framework which must therefore be locally damaged to accommodate such particles. The supporting zeolite, however, still appears to be highly crystalline and of a regular morphology; this supports the XRD data given in Figs. 2 and 3.

To investigate the formation of the cobalt particles, a sample of 10Co/Na–X was examined by STEM both before and after exposure to hydrogen gas. Fig. 5(*a*) and 5(*b*) show the micrographs of a sample of 10Co/Na–X after occlusion, but before reduction. From these images we see little evidence of particle formation for the occluded samples. After hydrogen reduction, however, the ultrafine particles of cobalt are easily visible by STEM [Fig. 6(*a*) and 6(*b*)]. In comparison with the 5Co/Na–X sample [Fig. 4(*a*) and 4(*b*)], there appears to be a greater concentration of metal particles present in the 10Co/Na–X sample, but, importantly, the sizes of these particles are still within the range 150–250 Å. This is consistent with the XRD data shown in Figs. 2 and 3, with the emergence of a broad line at 2θ *ca.* 44° characteristic of cobalt metal particles of diameter 150–250 Å and whose intensity (but not width) increases with increasing cobalt concentration.

The presence of cobalt particles with these characteristic dimensions was common through the range of concentrations up to 20Co/Na–X. STEM micrographs of the 20Co/Na–X (occluded/reduced) sample are shown in Fig. 7(*a*) and 7(*b*). As can be seen there is a considerably higher concentration of particles (once again with diameters in the 150–200 Å size range) than for the more lightly loaded samples. This is again consistent with the increase in intensity of the cobalt {111} reflection observed in the XRD pattern (Fig. 3).

The observed increase in the actual number of 150–250 Å particles with increasing cobalt loading, rather than an increase in the particle size, is consistent with a model of growth-arrested cobalt particles encapsulated in locally disrupted areas of the zeolite. The quantity of the zeolite thus damaged should increase with increasing cobalt loading. This is reflected in the XRD data which show a steady decrease in the intensity of the higher 2θ reflections from the host zeolite (which are the most sensitive to defects or disorder in the structure) as the cobalt loading is increased. However, we stress that the overall crystallinity of the resulting zeolite-loaded samples is still high (*e.g.* Fig. 7) and the overall morphology is similar to that of the pure zeolite.

From the data, it now seems clear that a high concentration of clusters and particles is present. A proportion of the particles may be accommodated in the supercage cavities of the zeolite having a characteristic dimension of *ca.* 13 Å. The larger particles (> 13 Å) can either be located in enlarged cavities or pores within the zeolite, which are produced by local distortions of the zeolite structure or on the external surface of the zeolite crystallite.

Magnetic susceptibility

The magnetic susceptibility data show clear qualitative differences in behaviour between the occluded and occluded/reduced samples. Both the XRD and STEM data for the occluded samples show no evidence of ultrafine metallic cobalt particles, but are consistent with the presence of intracrystalline phases of occluded cobalt nitrate. This is reflected in the magnetic susceptibility behaviour; representative data for the 10Co/

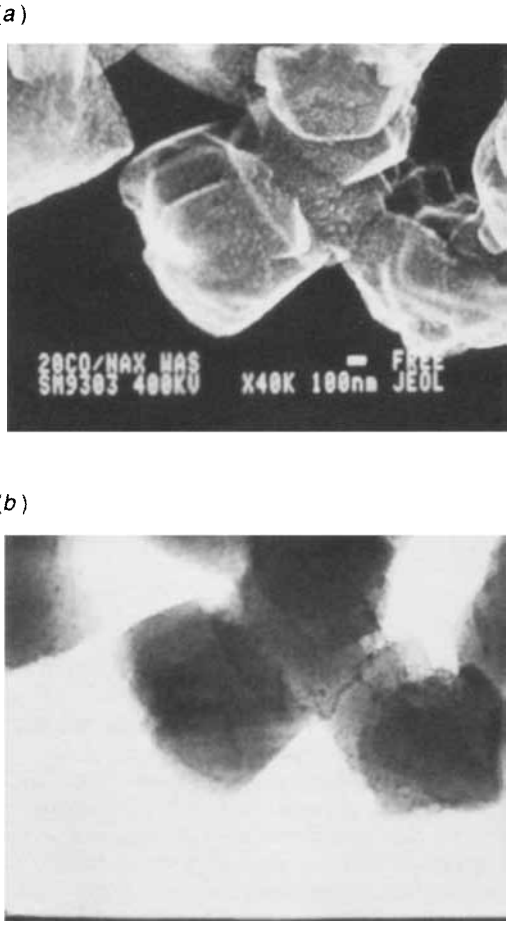

Fig. 7 (*a*) Scanning and (*b*) transmission electron micrograph of 20Co/Na–X(occluded/reduced)

Na–X(occluded) sample are given in Fig. 8(*a*) and 8(*b*). The magnetic properties of the occluded samples are in broad agreement with earlier susceptibility data[25] for cobalt ion-exchanged zeolites X and A, although the latter study only extended down to *ca.* 100 K. A plot of reciprocal susceptibility *versus* temperature for the (present) cobalt occluded sample is shown in Fig. 8(*b*); again this is consistent with a mixture of tetrahedral and octahedral cobalt(II) ions,[25] as one anticipates for cobalt(II) ions entrapped in specific lattice sites within the host framework. We note that there is clear evidence for magnetic interactions below 100 K, probably of a ferrimagnetic type. We are currently investigating this phenomenon in greater detail.

In contrast, all of the occluded/reduced samples showing clear evidence of ultrafine cobalt particles in both the XRD and STEM data exhibit the characteristic magnetic features associated with such systems.[26] In Fig. 9 we show a typical hysteresis loop (−0.1 to +0.1 T) observed during a magnetisation/demagnetisation cycle taken at 15 K. The loop is symmetrical about zero field. As indicated elsewhere,[26] this symmetry implies that no CoO was formed on the particle surfaces; again this is consistent with our structural data. The samples typically had a coercivity of *ca.* 0.05 T (at 15 K). All of these magnetic features indicate that certain of the cobalt particles are sufficiently large to exhibit ferromagnetic behaviour. A closer inspection of the magnetisation–field characteristics (Fig. 9) shows that the sample cannot be completely saturated at 15 K, and for fields up to 0.1 T. This finding suggests that the samples also contain a minor fraction of the cobalt particles sufficiently small to exhibit so-called 'superparamagnetic' behaviour.[27,28] High-field magnetisation studies are currently in progress to obtain the saturation magnetisation (*via* a $1/H$ extrapolation) up to 8 T. This lack of

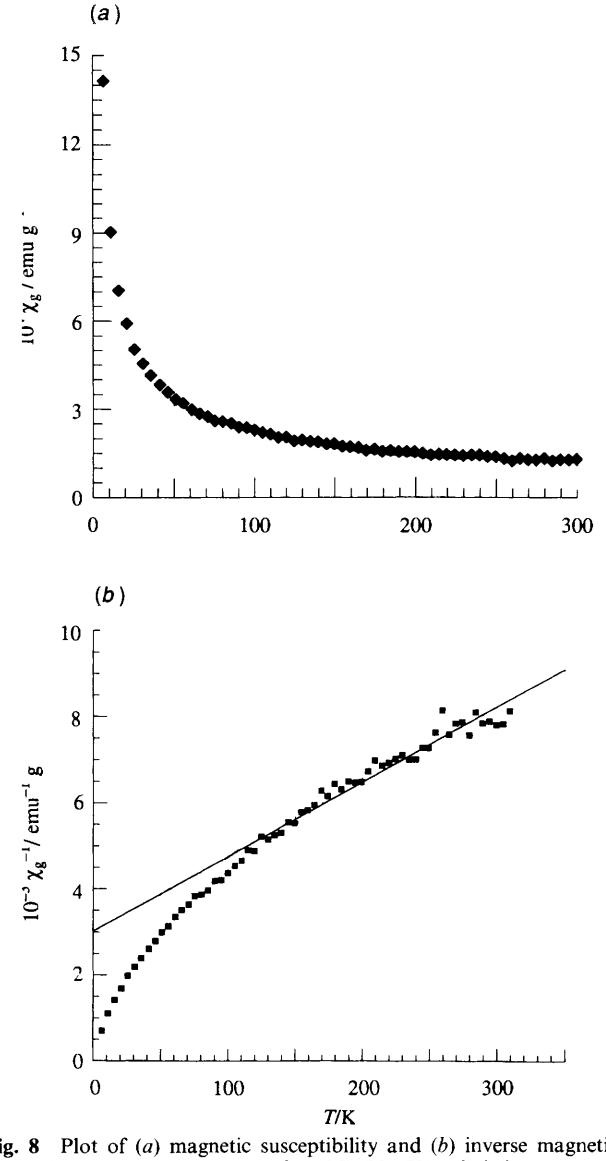

Fig. 8 Plot of (*a*) magnetic susceptibility and (*b*) inverse magnetic susceptibility *versus* temperature for 10Co/Na–X(occluded)

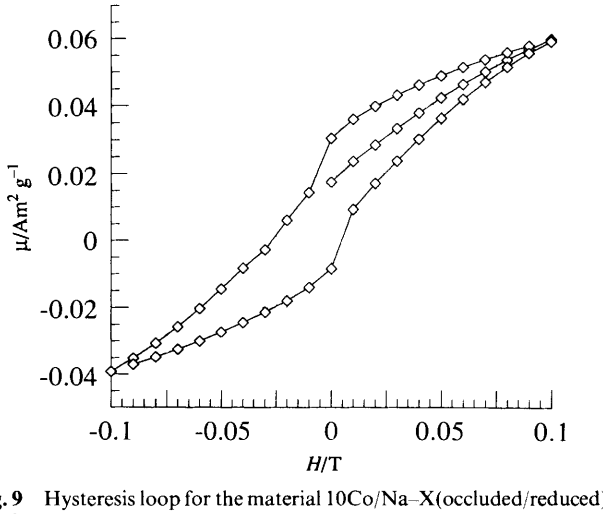

Fig. 9 Hysteresis loop for the material 10Co/Na–X(occluded/reduced) at 15 K

saturation leads one to conclude that the samples consist of particles of, broadly, two different size regions, a superparamagnetic and a ferromagnetic fraction. We arbitrarily set a demarcation at a particle size of *ca.* 50 Å to separate these two magnetic regimes; this value derives from earlier results of

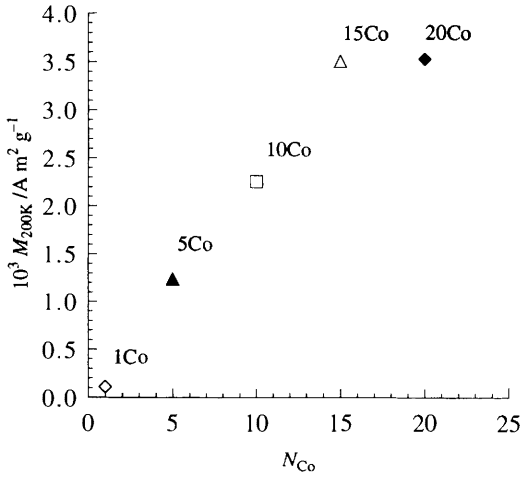

Fig. 10 Plot of magnetisation at 200 K (M_{200K}) *versus* the number of cobalt atoms per formula unit (N_{Co})

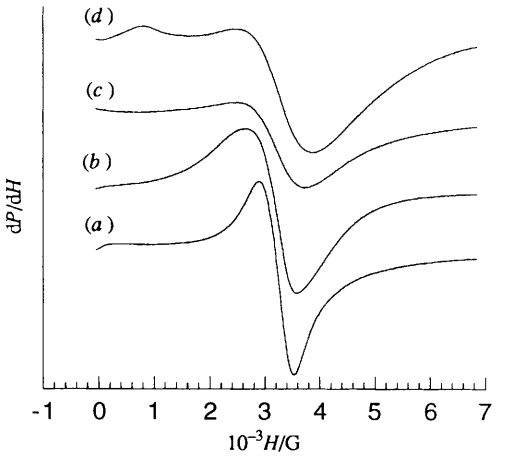

Fig. 11 ESR spectra taken at room temperature of samples 5Co/Na–X(occluded/reduced) to 20Co/Na–X(occluded/reduced) (*a*)–(*d*); G = 10^{-4} T

Klabunde and co-workers[28] on the magnetic properties of microemulsion-synthesised cobalt fine particles.

Our STEM and XRD data give direct evidence for cobalt particles in the range 150–200 Å. However, these techniques are not ideally suited for observing particles below *ca.* 50 Å, which may be the (interior) ultrafine particles responsible for the superparamagnetic behaviour hinted at by the magnetic investigations. What is clear, however, is that the majority of the particles are in the ferromagnetic 180–200 Å particle-size regime and that increasing the cobalt concentration *leads to higher concentrations of the same particle sizes; not to higher aggregates and larger particles.* It is proposed that the particle size is approximately independent of cobalt loading. Thus, additional cobalt occlusion and reduction leads simply to more particles, not larger particles, *i.e.* the sample retains the high dispersion of particles. In this case one anticipates a scaling relation for the ferromagnetic magnetisation, or moment, M_{200K} (taken at 200 K), at a given temperature, such that $M_{200K} \propto$ [Co], where [Co] is the weight fraction or, alternatively, the (nominal) number of cobalt atoms per formula unit. The SQUID data were normalised (by dividing by the mass of sample used) and are plotted against the concentration of cobalt atoms per formula unit, N_{Co}. Fig. 10 shows the variation of M_{200K} with cobalt atom concentration; the graph shows a steady increase in M_{200K} with increased cobalt concentration. It is evident that a larger moment is obtained when there is a greater concentration of cobalt present, as anticipated from the model outlined above. This behaviour is contrary to that experienced with metals supported on amorphous materials (*e.g.* alumina) where one always finds that a higher loading of metal particles leads to larger particles.[29]

Electron spin resonance

ESR spectra of 5Co/Na–X to 20Co/Na–X(occluded/reduced) were recorded at room temperature and are shown in Fig. 11. At low levels of cobalt loading, a strong resonance centred at $g \approx 2$ with intensity extending to zero field arises from ferromagnetic resonance of the particles. The approximate form of the resonance is maintained to the high levels of cobalt loading, but there is an increase in the intensity of the signal at low field in comparison to the signal at $g \approx 2$. In addition, the resonance close to $g \approx 2$ broadens with increasing metal concentration. The spectra are similar to those reported previously for fcc cobalt particles.[30,31] The signal strength, measured as the double integral of the recorded spectrum, increases with cobalt loading; once again this is consistent with the structural and magnetic data which point to an increasing number of ultrafine cobalt particles.

Conclusion

We hope to have demonstrated the clear potential of zeolites as templates or host matrices in the synthesis of magnetic composite materials. The ability to prepare ultrafine metal particles, with high dispersion, throughout a range of compositions, sets these systems apart from amorphous supports (such as alumina or silica).[29,32] The picture to emerge identifies the characteristic cavity and channel structure of zeolites as crucial to the generation of these ultrafine particles. It is recognised that the co-ordination chemistry requirements of the occluded cobalt nitrate (Fig. 1) dictate that the cobalt(II) ions will be most stable in the smaller sodalite cages (or in the hexagonal prisms) where they co-ordinate better with oxygen ions of the cage walls. Indeed, earlier XRD studies have confirmed that transition-metal ions tend to migrate from supercages towards smaller cages at elevated temperatures.[33] By smaller cages we mean either 'sodalite' cages or 'hexagonal prisms'.[34]

After initial reduction of cations located in the sodalite cages (and/or the hexagonal prisms), the atomic species so formed will migrate to the supercage to form higher aggregates. Both atomic and ionic migration is known in zeolites, but activation barriers for migration of neutral atoms (and presumably clusters) are much lower. There is a clear thermodynamic driving force for the atomic clusters to grow by aggregation to form larger clusters and particles by the coalescence of smaller particles. Aggregation to form clusters and particles larger than the supercage dimensions (> 13 Å) would ensure that these particles are located in a locally destroyed region of the zeolite crystallite. In fact, enlarged supercages of this sort have been observed directly in TEM studies of platinum clusters in zeolites.[32] This may explain our observations that the samples with the highest metal content still retain a high dispersion, with no clear signs of sintering to produce enlarged particles. Here, the smaller primary particles in the cobalt-loaded samples can rapidly migrate through the characteristic cavity and channel structure of the zeolite over large distances. The critical aggregation process, here taken as the growth event which takes cobalt particles above the characteristic dimensions of the supercage (*ca.* > 13 Å), effectively triggers an 'impact' nucleation site within a locally enlarged or destroyed structure of the zeolite matrix.[29] Clearly, a certain proportion of the freely diffusing atoms and clusters will completely traverse the supercage labyrinth without encountering any such nucleation site. These will migrate to the exterior of the crystallite (the surface) where the final nucleation site will be initiated when the growing particle exceeds the host supercage dimension.

What sets the present materials apart from both their amorphous[29] (support) counterparts and the ion-exchange route[17] appears to be the homogeneous dispersion of the resulting ultrafine particles. The physical dimensions of such cobalt particles (*ca.* 150–200 Å) clearly necessitate a local distortion/disruption or even destruction of the host zeolite. However, further aggregation to particles larger than these dimensions does not appear to take place (under the present synthetic conditions). Furthermore, the overall crystallinity and morphology of the micron-sized host crystallites remains virtually intact (*e.g.* Figs. 4–7).

The high spatial dispersion of the 'precursor' nitrate and oxide forms of cobalt, and the high concentrations of such occluded species, may exert a profound influence on the initiation, growth and nucleation process taking place within the host zeolite. All of these findings indicate that this synthetic route, coupled with the characteristic nanoscale cavity and channel structure of the zeolite, may allow one to 'engineer' chemically the nano-fabrication, in large quantities, of magnetic and other technologically important ultrafine particles.

Acknowledgements

We acknowledge the EPSRC and Alcan Chemicals Ltd. for their financial support. We also wish to thank Dr. K. Evans (Alcan Chemicals Ltd.) and Professor I. R. Harris (School of Metallurgy and Materials) for their support and encouragement. P. A. A. is a Royal Society University Research Fellow. This work has been carried out under the auspices of the Centre for Electronic and Magnetic Materials (CEMM), the University of Birmingham.

References

1 *Nanostruct. Mater.*, 1993, **3(1–6)**.
2 *Nanostruct. Mater.*, 1993, **6(1–8)**.
3 S. Gangopadhay, G. C. Hadjipanayis, B. Dale, C. M. Sorenson and K. J. Klabunde, *Nanostruct. Mater.*, 1992, **1**, 77.
4 D. D. Awschalom and D. P. DiVincenzo, *Phys. Today*, 1995, **48**, 43.
5 D. Jiles, *Introduction to Magnetism and Magnetic Materials*, Chapman & Hall, London, 1st edn., 1991.
6 R. D. Shull, R. D. Michael and J. J. Ritter, *Nanostruct. Mater.*, 1993, **2**, 205.
7 H. A. Davies, A. Manaf, M. Leonowicz, P. Z. Zhang, S. J. Dobson and R. A. Buckley, *Nanostruct. Mater.*, 1993, **2**, 197.
8 S. Gangopadhay, G. C. Hadjipanayis, C. M. Sorenson and K. J. Klabunde, *Nanostruct. Mater.*, 1992, **1**, 449.
9 R. D. Shull, R. D. Michael and J. J. Ritter, *Nanostruct. Mater.*, 1992, **1**, 83.
10 E. Matijevic, *Mater. Res. Bull.*, 1989, **14**, 19.
11 R. P. Andres, R. S. Averbach, W. L. Brown, L. E. Brus, W. A. Goddard III, A. Kaldor, S. G. Louie, M. Moskovitz, P. S. Peercy, S. J. Riley, R. W. Siegel, F. Spaepen and Y. Wang, *J. Mater. Res.*, 1989, **4**, 704.
12 R. W. Siegel, *Nanostruct. Mater.*, 1993, **3**, 1.
13 *Stud. Surf. Sci. Catal.*, 1982, **12**.
14 *Stud. Surf. Sci. Catal.*, 1982, **12**, 71.
15 J. B. Uytterhoven, *Acta Phys. Chem.*, 1978, **24**, 53.
16 Kh M. Minachev and Ya I. Isakov, *ACS Monogr.*, 1976, 171.
17 J. C. Kim and I. S. Woo, *Appl. Catal.*, 1988, **39**, 107.
18 R. Harjula, J. Lehto, J. H. Pothuis, A. Dyer and R. P. Townsend, *J. Chem. Soc., Faraday Trans.*, 1993, **89**, 971.
19 R. M. Barrer, *J. Inclusion Phenom.*, 1983, **1**, 105.
20 R. M. Barrer and W. M. Meier, *J. Chem. Soc.*, 1958, 299.
21 J. A. Rabo and P. H. Kasai, *Prog. Solid State Chem.*, 1975, **9**, 1.
22 *NBS Monogr. US*, 1965, **25**.
23 M. E Mohenry, S. A. Majetich, J. O. Artman, M. DeGruef and S. W. Staley, *Phys. Rev. B*, 1994, **49**, 11358.
24 H. P. Klug and L. E. Alexander, *X-Ray Diffraction Procedures for Polycrystalline and Amorphous Materials*, Wiley, New York, 2nd edn., 1974.
25 T. A. Egerton, A. Hagan, F. S. Stone and J. C. Vickerman, *J. Chem. Soc., Faraday Trans. 1*, 1972, **68**, 723.
26 J. P. Chen, C. M. Sorenson, K. J. Klabunde and G. C. Hadjipanayis, *Phys. Rev. B*, 1995, **51**, 11527.
27 C. P. Bean and J. D. Livingstone, *J. Appl. Phys.*, 1959, **30**, 1205.
28 J. P. Chen, K. M. Lee, K. J. Klabunde and G. C. Hadjipanayis, *J. Appl. Phys.*, 1994, **75**, 5876.
29 W. M. H. Sachtler, M. S. Tzon and H. J. Jiang, *Solid State Ionics*, 1988, **26**, 71.
30 C. P. Bean, J. D. Livingstone and D. S. Rodbell, *Acta Metall.*, 1957, **5**, 682.
31 P. M. Valetsky, S. P. Solodovnikov and R. A. Register, *J. Mater. Chem.*, 1995, **5**, 1197.
32 F. Schmidt, *Stud. Surf. Sci. Catal.*, 1982, **12**, 191.
33 P. Gallezot, *Catal. Rev. Sci. Eng.*, 1979, **20**, 121.
34 W. J. Mortier, *Compilation of Extra Framework Sites in Zeolites*, Butterworths, London, 1982.

Received 24*th October* 1995; *Paper* 5/07159C